
Research Article

Neutral Electrolyzed Water Decreases Triple-Negative Breast Cancer Cell Viability, Clonogenic Survival, Adhesion, Migration, and 3-D Spheroid Growth.

Ariana Cabrera-Licona^{1,4}, Juan Paz-García², Oscar F. Beas Guzmán^{3,4}, Iván Delgado-Enciso^{3,4}, Brenda A. Paz-Michel^{1*}

Abstract

Neutral Electrolyzed Water (NEW) is a type of electrolyzed oxidizing water that exhibits health-promoting properties in humans, as evidenced by its positive effects on wound repair, encompassing mild to severe injuries, modulation of both local and systemic inflammatory processes and, more recently, in the prevention and control of infections and symptoms associated with COVID-19. Concerning its potential in cancer treatment, there have been no prior direct investigations into its effects on cancer cells. In this study, we examined NEW-induced alterations in triple-negative breast cancer hallmarks, including cell proliferation, survival, migration, and adhesion, in 2-D cultures. Additionally, we assessed its impact on cell growth in 3-D cultures and their reversion. The results revealed that NEW containing 0.002% reactive oxygen species and chlorine affected the cell viability of the MDA-MB-231 line, in a concentration-dependent manner, with an IC₅₀ of 28.95% v/v (R²= 0.9587; 95% IC= 27.87 to 30.07) at 96 hours of treatment. Treatment with 50% v/v resulted in a significant reduction in clonogenic survival (up to 96%), migration at 24 hours (up to 98%), and adhesion (up to 83%). Similarly, NEW decreased the growth of 3-D cultures in a concentration-dependent manner and, at 50% v/v, completely inhibited their reversion to 2-D. These findings parallel those obtained with the chemotherapy doxorubicin, the standard treatment for this type of cancer. The results suggest that NEW may represent a novel therapeutic option against this aggressive cancer type for which there is currently no specific therapy, warranting further exploration and attention.

Keywords: Neutral Electrolyzed Water; breast cancer; triple-negative breast cancer; MDA-MB-231 cells.

Introduction

Neutral Electrolyzed Water (NEW), also known as neutral oxidant, is obtained by mixing the water produced at the anode and cathode during the electrolysis of a NaCl solution [1, 2]. Its active components are reactive chlorine and oxygen species, with primary active chlorine species comprising free chlorine, hypochlorous acid, and sodium hypochlorite. Concurrently, major reactive oxygen species include superoxide anion, hydrogen peroxide, ozone, and chlorine dioxide [1, 3]. The resultant NEW has a pH range of 6.8-7.4, an oxide-reduction potential (ORP) of 750-900 mV, and an osmolarity of 13 mOsm/kg [1]. These physicochemical attributes confer NEW with broad-spectrum bactericidal, fungicidal and virucidal properties [1, 2, 4]. They also make it tissue-friendly and non-corrosive, which renders it applicable for diverse purposes, including the disinfection of vegetables, fruit, animal-

Affiliation:

¹Department of Research and Industrial Property, Esteripharma S.A. de C.V., 50450, Estado de México, México

²Union Hospital Center, Villa de Álvarez, 28970, Colima, México

³School of Medicine, Colima University, 28040, Colima, Mexico

⁴Department of Research, Cancerology State Institute, Colima State Health Services, 28085, Colima, Mexico

*Corresponding author:

Brenda A. Paz-Michel, Esteripharma, S.A. de C.V., Libramiento Jorge Jiménez Cantú OTE 412, Colonia 2 de abril, 50450, Estado de México, México

Citation: Ariana Cabrera-Licona, Juan Paz-García, Oscar F. Beas Guzmán, Iván Delgado-Enciso, Brenda A. Paz-Michel. Neutral Electrolyzed Water Decreases Triple-Negative Breast Cancer Cell Viability, Clonogenic Survival, Adhesion, Migration, and 3-D Spheroid Growth. *Journal of Cancer Science and Clinical Therapeutics*. 8 (2024): 83-94.

Received: February 08, 2024

Accepted: February 14, 2024

Published: February 28, 2024

derived foods (e.g. meat, eggshells, and seafood), as well as hospital settings and medical devices [5-9]. Animal model studies have established that NEW with these physicochemical characteristics is not toxic to mucous membranes, the dermis or the epidermis, even when administered systemically [10-12]. Although within the realm of human health, NEW is particularly used in wound healing, it has also been linked to the modulation of the immune response in conditions such as peritonitis, inflammatory cervical lesions, rheumatoid arthritis, nephrotoxicity, Chagas disease, and COVID-19 [13-18]. Researchers have postulated that NEW could redirect the proinflammatory response towards an anti-inflammatory and reparative one through Redox signaling. Nevertheless, the specific mechanisms of action of NEW in these or other pathologies remain to be elucidated. Triple-negative breast cancer (TNBC) is a specific subtype of breast cancer that predominantly affects premenopausal young women under 40 years old, is highly invasive and metastatic, and has a very poor overall prognosis, with an average relapse occurring within 5 years post-surgery [19, 20]. TNBC tumors lack expression of estrogen receptors, progesterone receptors, and human epidermal growth factor receptors. Consequently, they are impervious to endocrine therapy or HER2 treatment [19, 20]. While chemotherapy serves as the primary systemic treatment, its effectiveness as a conventional postoperative adjuvant is limited [19, 20]. The use of immunotherapy and legacy drugs based on molecular typing of this cancer and its subtypes is currently being explored [20]. However, numerous challenges persist, underscoring the present clinical imperative for the development of novel and readily accessible treatment strategies.

To our knowledge, no research has been conducted on the effects of neutral electrolyzed water on cancer cells, specifically with regard to triple-negative breast cancer cells. A study by Saitoh et al. demonstrated that neutral pH hydrogen-enriched electrolyzed water could inhibit colony formation and cell proliferation in human tongue squamous cell carcinoma-derived cell line HSC-4, as well as the proliferation and invasion of human fibrosarcoma HT-1080 cells [21]. Nevertheless, it is imperative to emphasize that the water utilized in this investigation exhibited distinct physicochemical characteristics in comparison to NEW. Specifically, the water used in the aforementioned study was electrolyzed reducing water with negative values of Oxidation-Reduction Potential (ORP) ranging from -590 to -104 mV, whereas the oxidizing ORP of NEW ranges from 750 to 900 mV. Consequently, a direct comparison between these waters is not warranted. Similarly, despite its chemical distinctions, basic electrolyzed water has garnered more extensive research supporting its effects on various types of cancer cells, and it has even demonstrated the ability to delay mammary tumor growth in *in vivo* models [4, 22]. In this context, it is crucial to ascertain whether NEW exerts effects

on the hallmarks of cancer, given its potential as an accessible therapy for systemic or local administration without causing harm to non-tumor cells. In this preliminary investigation, we assessed the impact of NEW on the MDA-MB-231 cell line, representative of a mesenchymal stem-like triple-negative breast cancer subtype. Our study assessed NEW-induced changes in cell viability, clonogenic survival, migration, and adhesion in 2-D cultures of MDA-MB-231 cells. Additionally, we explored whether NEW affects the growth of these cells in 3-D cultures and their reversion to 2-D monolayers. The results obtained clearly showed that NEW impacts the hallmarks of cancer in a concentration-dependent manner. Notably, at a concentration of 50% v/v in the medium, neutral electrolyzed water led to almost complete inhibition of these characteristics, mirroring the effects of the chemotherapeutic doxorubicin. Despite the observed shorter-term effects, especially on migration and adhesion, these findings imply that NEW could emerge as a novel therapeutic option for this aggressive and metastatic cancer type, which currently lacks a specific therapy. Therefore, further exploration and focused attention on this potential therapeutic avenue are warranted.

Materials and Methods

NEW Characteristics and Treatments

The NEW employed in all the experiments exhibited the following chemical characteristics: 0.002% reactive oxygen and chlorine species, a pH range of 6.5-7.5, and an ORP of 750–900 mV (Esteripharma S.A de C.V). For treatments, NEW was utilized in varying concentrations of 10%, 20%, 30% 40% and 50% (v/v) in Dulbecco's Modified Eagle Medium F-12 (DMEM/F-12, Gibco, Thermo Fisher) supplemented with 1% fetal bovine serum (FBS) (Gibco, Thermo Fisher) and 1x penicillin/streptomycin (Antibiotic-Antimycotic 100x, Gibco, Thermo Fisher). The positive control comprised 2 μ M doxorubicin (experimental determined IC50 for 48 hrs), while the negative control consisted of DMEM medium without NEW.

Cell Culture

MDA-MB-231 cell line (ATCC: HTB-26TM, Manassas, VA, USA) were maintained in DMEM/F-12 supplemented with 10% (v/v) FBS and 1x penicillin/streptomycin. Cells were incubated at 37 °C in 95% air in a humidified incubator with 5% CO₂. 0.25% Trypsin-EDTA Solution (Gibco) was used for cell harvesting during subculturing.

Cell Viability Assay/Cytotoxicity

Triple-negative breast cancer cells MDA-MB-231 were seeded in a 96-well TC-treated flat-bottom microplate (Corning®) at a density of 1×10^4 cells/well in DMEM/F-12 medium supplemented with 10% FBS and incubated for 24 hours in a 5% CO₂ atmosphere at 37°C. Subsequently, the medium was replaced with the designated treatment in a final volume of 100 μ L/well, following the previously

described protocol. Cells were incubated for 96 hours in a 5% CO₂ atmosphere at 37°C. After treatment, the medium was removed, and the cells were incubated with 1x Alamar Blue™ Cell Viability Assay Reagent (Sigma-Aldrich) in phenol red-free medium for 4 hours. Optical density was determined at the respective excitation and emission wavelength of 570-600 nm using a microplate reader (iMark, Bio-Rad). The cytotoxic index was calculated as: $100 - [(OD \text{ value experimental} - OD \text{ value blank}) / (OD \text{ value control} - OD \text{ value blank}) \times 100\%]$. The IC₅₀ was determined through a non-linear regression curve fit analysis in GraphPad Prism (San Diego, USA). Images were captured using the inverted microscope AE31 EPI (Motic) coupled to the Moticam Pro 252A camera and the Motic Images Plus 2 software.

Assessment of Membrane Permeability Using a Modified Trypan Blue Exclusion Assay

Monolayers of MDA-MB-231 cells reaching approximately 70% confluence in a 24-well TC-treated plate were incubated for 96 hours with the designated treatment. Subsequently, the medium was carefully removed and cells were subjected to *in vivo* staining using 0.4% trypan blue in PBS for 10 minutes. The dye was then gently removed, and the cells were fixed for 15 minutes with buffered formalin. Images were captured using the inverted microscope AE31 EPI (Motic) coupled to the Moticam Pro 252A camera and the Motic Images Plus 2 software.

Clonogenic Assay

MDA-MB-231 cells were seeded in a 96-well TC-treated flat-bottom microplate (Corning®) at a density of 1x10⁴ cells/well in DMEM-supplemented medium and incubated for 24 hours in a 5% CO₂ atmosphere at 37°C. The medium was then removed and a final volume of 100 μL of the treatment medium was added, as previously described. Cells were incubated for 96 hours in a 5% CO₂ atmosphere at 37°C. Following treatment, the medium was removed, cells were washed with warm sterile 1x PBS (pH 7.4), harvested with 0.25% trypsin-EDTA (Gibco, Thermo Fisher), stained with trypan blue (SigmaAldrich), and counted. Subsequently, 200 cells from each treatment, suspended in 500 μL of DMEM/F-12 supplemented with 10% FBS and 1x penicillin/streptomycin, were seeded in a 24-well TC-treated plate, in triplicate. The plates were incubated for 14 days, with medium changes every 5 days. At the conclusion of the incubation period, the cells were fixed for 15 minutes with buffered formalin, and stained with 0.4% crystal violet for 45 minutes, washed with H₂Odest to remove excess dye, and images were captured. Colonies were counted, and the percentage of survival was calculated as follows: $(\text{number of colonies in treatments} \times 100) / \text{number of colonies in control}$.

Wound Healing Assay

Monolayers with approximately 90% confluence were

subjected to a scratch assay using a 200 μL tip, followed by a wash with warm sterile 1x PBS (pH 7.4) to remove unattached cells. Subsequently, serum-free treatment medium, and cells were incubated for 96 hours. Images were captured at 24, 48, 72 and 96 hours using the inverted microscope AE31 EPI (Motic) coupled to the Moticam Pro 252A camera and the Motic Images Plus 2 software to monitor cell migration into the wounded area. The images were analyzed with TScratch software [23], and the percentage of area reduction was calculated as follows: $100 - [(area_{Tx} \times 100) / area_{T0}]$, where Tx= the area at 24, 48, 72 or 96 hours, and T0 represents the area at the beginning of the follow-up.

Adhesion Assay

MDA-MB-231 cells were seeded in a 24-well TC-treated plate at a density of 2x10⁴ cells/well in DMEM-supplemented medium and incubated for 24 hours in a 5% CO₂ atmosphere at 37°C. Subsequently, cells were treated with NEW for 96 hours, as previously described. Both adherent and suspended cells were harvested, stained with trypan blue (SigmaAldrich) and counted. The suspended cells were then reseeded in a 24-well TC-treated plate to analyze their adherence. After an additional 24 hours, both attached and suspended cells were harvested, stained with trypan blue (SigmaAldrich) and counted. Images were captured using the inverted microscope AE31 EPI (Motic) coupled to the Moticam Pro 252A camera and the Motic Images Plus 2 software. The percentages of adhesion and dead cells were calculated for each treatment condition.

3D Spheroid Cultures and Reversion

Spheroids were generated employing the liquid overlay technique, with a non-adhesive surface created by a thin coating of agarose [24, 25]. In advance, the 96-well plates were coated with 50 μL of 1% agarose in water and allowed to solidify for 1.5 hours. Subsequently, 5000 cells/100 μL of DMEM-supplemented medium were seeded per well and incubated for 72 hours in a 5% CO₂ atmosphere at 37°C. Following incubation, spheroids were treated with NEW for 96 hours, adhering to the previously described protocol. At the conclusion of the treatment period, the spheroids were carefully transferred to a 96-well TC-treated plate and incubated for 24 hours before replacing the medium with fresh medium. The plates were then incubated for an additional 72 hours. Images were captured at the initiation and conclusion of NEW treatments, as well as at the conclusion of the reversion assay, using the inverted microscope AE31 EPI (Motic) coupled to the Moticam Pro 252A camera and the Motic Images Plus 2 software. The spheroid area was measured with ImagenJ software, and changes in the percentage of growth were calculated as: $100 - [(area_{T96} \times 100) / area_{T0}]$.

Statistical Analysis

The results are presented as mean ± standard deviation (SD). For the cell viability and 3D spheroid cultures assays, the outcomes were averaged over three independent experiments with 10 replicates per experiment. For the clonogenic assay, adhesion assay, and wound healing assay, the results were averaged over three independent experiments, each with three replicates per experiment. Group differences were assessed using a one-way ANOVA statistical test with Tukey's Post Hoc. All statistical analyses were conducted using GraphPad Prism version 6.0 for Windows (GraphPad Software, San Diego, California USA, www.graphpad.com). Statistical significance at P values <0.0001, <0.001, <0.01, <0.05 is indicated with the respective symbols in the Figures.

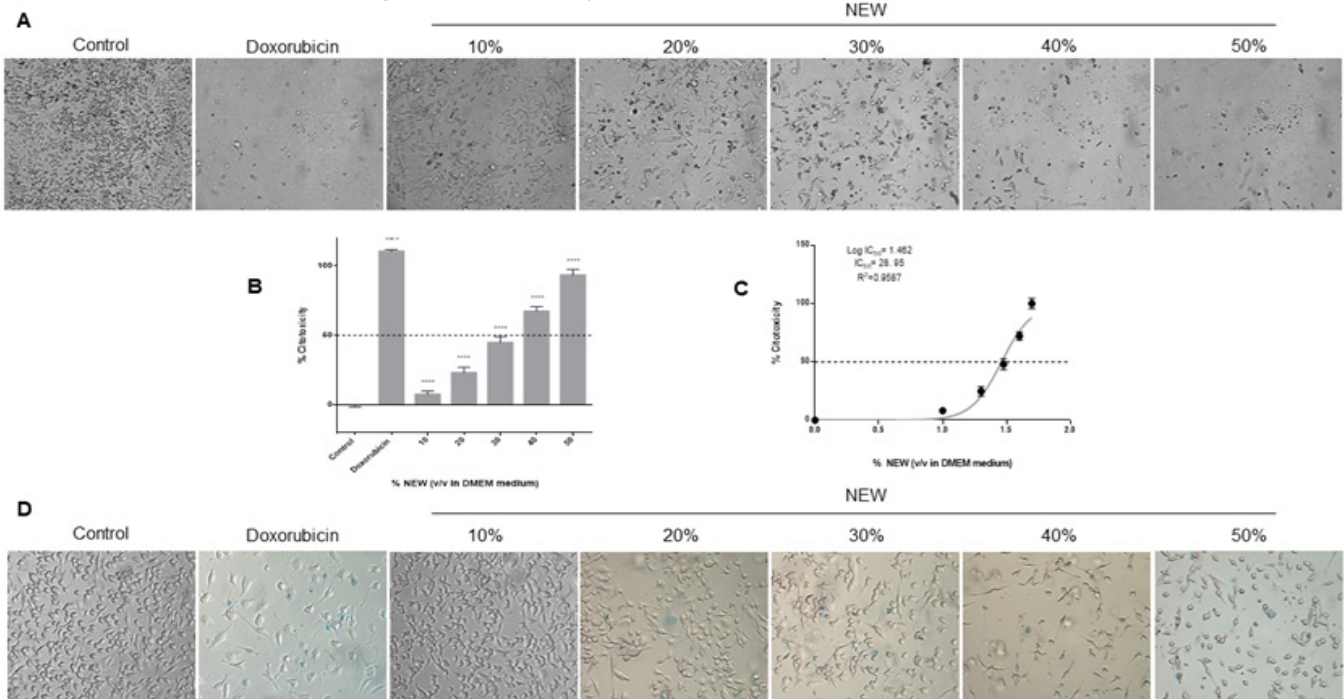
Results

NEW Had a Cytotoxic Effect Over MDA-MB-231 Cells

Treatment with neutral electrolyzed water induced notable morphological changes in MDA-MB-231 cells, evident even at the lowest concentration of 10% v/v in DMEM (Figure 1 A). A discernible reduction in cell density was observed in the monolayers relative to the control, with changes becoming more pronounced as the percentage of NEW in the culture medium escalated. Additionally, cells underwent a transition

from their typical fibroblast-like shape to a less elongated and even round morphology, devoid of protrusions, particularly evident at higher concentrations of NEW, ranging from 40-50% v/v (Figure 1). Cells treated with NEW at 50% v/v in DMEM exhibited morphological and cell density alterations akin to cells treated with 2 μM doxorubicin (experimental IC₅₀) after 96 hours of exposure. In both conditions, few cells remained adherent, displaying a rounded morphology. Quantification of the cytotoxic effect of NEW, using the chemotherapeutic drug doxorubicin as a reference, revealed a dose-dependent response. Treatments with 30%, 40%, and 50% of NEW in DMEM demonstrated the highest percentages of cytotoxicity with values of 44.85%±4.279, 64.84%±3.328 and 90.14%±4.161, respectively (Figure 1B). The half maximal inhibitory concentration calculated for NEW was 28.95% v/v (CI 95%= 27.87 to 30.07 and R²= 0.9587) (Figure 1C). It is noteworthy that the 60% concentration was also tested, revealing 100% inhibition/cytotoxicity on MDA-MB-231 cell monolayers (data not shown). To investigate whether the NEW-mediated cell death mechanism involves cell membrane damage, an assessment of membrane permeability was conducted using an exclusion assay (Figure 1D). Despite the observed morphological changes, no increase in the number of staining-positive cells was noted in any of the NEW treatments assessed when compared with doxorubicin-treated monolayers.

Figure 1: NEW had a cytotoxic effect on MDA-MB-231 cells



A) Micrographs show shortening and substrate detachment in cells treated with 10%, 20%, 30%, 40%, and 50% NEW for 96 h. Magnification x 10. B) The graph shows that NEW had a cytotoxic effect directly proportional to concentration. The 50% v/v concentration had a similar effect to doxorubicin, which induced 100% cell death. C) The graph shows the maximum mean inhibitory concentration of NEW on MDA-MB-231 cells, which was estimated to be 28.95% v/v. D) The micrographs show the trypan blue positive cells in each NEW treatment. With all the concentrations tested, the number of staining-positive cells was minimal. P values correspond to significant differences compared to control, DMEM medium only, **** p<0.001.

A) Micrographs show shortening and substrate detachment in cells treated with 10%, 20%, 30%, 40%, and 50% NEW for 96 h. Magnification x 10. B) The graph shows that NEW had a cytotoxic effect directly proportional to concentration. The 50% v/v concentration had a similar effect to doxorubicin, which induced 100% cell death. C) The graph shows the maximum mean inhibitory concentration of NEW on MDA-MB-231 cells, which was estimated to be 28.95% v/v. D) The micrographs show the trypan blue positive cells in each NEW treatment. With all the concentrations tested, the number of staining-positive cells was minimal. P values correspond to significant differences compared to control, DMEM medium only, **** p<0.001.

NEW Decreased the Survival of MDA-MB-231 Cells

Following 96 hours of treatment with neutral electrolyzed water, MDA-MB-231 cells were recovered and reseeded at a low density to assess the impact of NEW on their clonogenic survival. The ability of cells to generate colonies was dose-dependently affected by the treatment (Figure 2A). In concordance with the calculated IC₅₀ value, the number of colonies formed by cells treated with 30% v/v NEW in DMEM decreased by approximately half compared to the control, and only a few colonies formed from those treated with 50% NEW. The calculation of survival percentages revealed that treatment with 30% NEW resulted in a value of 42.47 ± 4.745, 40% had 21.92 ± 2.373, and 50% had 4.110 ± 0. In other words, treatment with NEW decreased colony

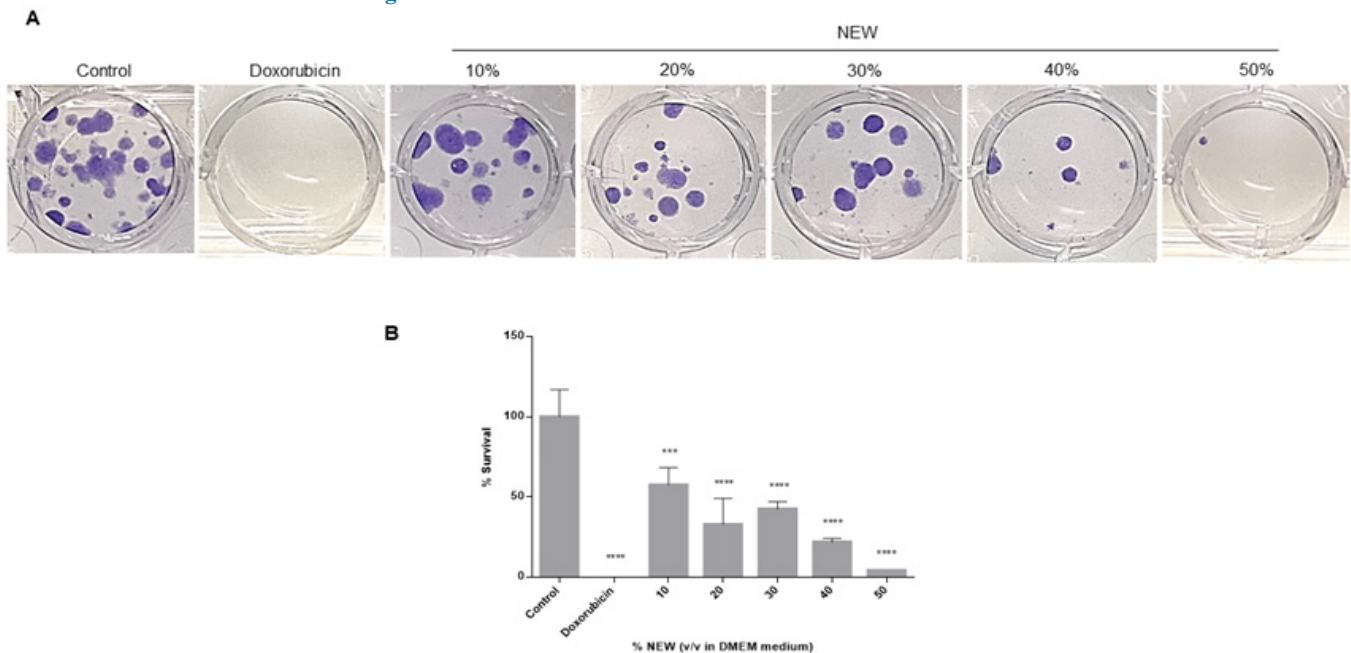
formation by approximately 60% for the 30% concentration and by 80% and 96% for the 40% and 50% concentrations, respectively (Figure 2B). In comparison, treatment with the chemotherapeutic agent exhibited an efficiency of 100% (Figure 2A, B).

A) Images correspond to the number of colonies formed by cells seeded after exposure to NEW, doxorubicin, or medium for 96 h, incubated for 14 days and stained with crystal violet. B) Quantification of colonies showed that clonogenic survival decreases as the concentration of NEW in the medium increases, by almost half at the 30% concentration, and close to 0 at the 50% concentration. P values correspond to significant differences compared to control, DMEM medium only, *** p<0.01, **** p<0.001.

NEW Inhibited the Migration of MDA-MB-231 Cells

The impact of NEW on the migration of triple-negative breast cancer cells was monitored over a time span of 24 to 96 hours to discern any effect related to cell death rather than a direct impact on cell migration (Figure 3). At 24 hours, area reduction was comparable for control conditions, doxorubicin treatment, and cells treated with 10% NEW (Figure 3A), displaying values of 20.42% ± 0.6825, 20.07% ± 0.8772 and 22.29% ± 1.469, respectively, with no statistical differences among them. Notably, the 20% concentration exhibited a slightly higher percentage of area reduction, above the control mean, recording a value of 23.99% ± 1.469 (p=0.0069) (Figure 3B). However, concentrations of 30%, 40%, and 50%

Figure 2: NEW decreased the survival of MDA-MB-231 cells



A) Images correspond to the number of colonies formed by cells seeded after exposure to NEW, doxorubicin, or medium for 96 h, incubated for 14 days and stained with crystal violet. B) Quantification of colonies showed that clonogenic survival decreases as the concentration of NEW in the medium increases, by almost half at the 30% concentration, and close to 0 at the 50% concentration. P values correspond to significant differences compared to control, DMEM medium only, *** p<0.01, **** p<0.001.

of NEW in the medium resulted in a minimal, statistically significant, area reduction compared to the control. For the 30% concentration, area reduction was $15.34\% \pm 1.344$ ($p=0.0003$); for the 40%, it was $3.134\% \pm 1.447$ ($p<0.0001$); and for the 50%, it was $1.644\% \pm 0.4730$ ($p<0.0001$) (Figure 3B). At 48 hours of incubation, the scratch area exhibited a decreasing trend in the control conditions ($28.93\% \pm 5.521$), doxorubicin ($27.40\% \pm 0.6673$), 10% ($27.45\% \pm 0.6131$), and 20% NEW ($30.23\% \pm 1.285$), without significant differences among them. A reduction in the area was also observed at the 30% ($20.63\% \pm 2.581$), 40% ($12.47\% \pm 3.015$), and 50% ($2.846\% \pm 2.208$) concentrations, compared to the 24-hour values. However, these concentrations maintained a significant difference with the 48-hour control and doxorubicin, with a P value of 0.0119 for 30%, and P values of <0.0001 for 40% and 50% v/v of NEW (Figure 3B). After 72 hours of treatment, the scratch area reduction tendency persisted in the control cells but decreased in the cells treated with the chemotherapeutic, with an area reduction percentage of $35.43\% \pm 2.072$ vs $28.83\% \pm 1.634$, respectively, and a P value of 0.0453. For NEW concentrations of 10% and 20%, the values of the scratch area reduction were similar to those of the control at this follow-up time, $33.17\% \pm 0.8372$ and $33.77\% \pm 1.506$, respectively, without statistical differences between them. Conversely, treatment with 30% NEW had a similar value to doxorubicin, $26.37\% \pm 3.080$ vs $28.83\% \pm 1.634$ for the chemotherapeutic; however, the statistical difference between NEW treatment and control was greater, with a P value of 0.0056. At concentrations of 40% and 50% of NEW, the scratch area remained broader compared to other tested conditions but smaller than the values observed at 48 hours,

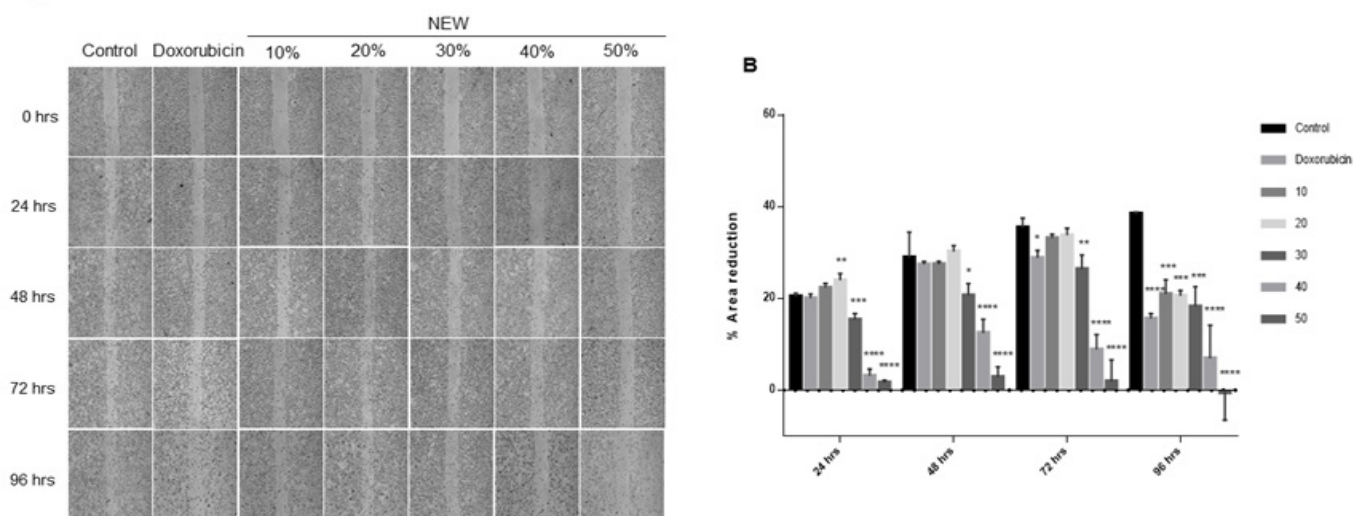
as shown in the graph. The monolayer treated with 40% NEW exhibited an area reduction of $8.866\% \pm 3.212$, demonstrating a statistically significant difference from the control greater than 0.0001. Similarly, at a 50% concentration, the percentage of area reduction was $1.901\% \pm 4.708$ (Figure 3B).

Finally, at 96 hours, all tested treatment conditions exhibited a migration area reduction compared to the control. This reduction tendency persisted until the scratch was completely closed, and all differences were statistically significant (Figure 3B). Notably, the 50% concentration of NEW yielded negative values, indicating an increase in the scratch area due to cell detachment. Furthermore, it is noteworthy that when the values throughout the follow-up were compared with doxorubicin, concentrations of 30%, 40% and 50% were more effective in inhibiting cell migration at shorter times. The 30% concentration exhibited a significant difference at 24 hours, with a P value of 0.0007, and 0.0430 at 48 hours. The 40% concentration showed a difference at 24, 48 and 72 hours, with P values exceeding 0.0001. Meanwhile, the 50% NEW concentration demonstrated a significant difference with doxorubicin at all follow-up times, with P values surpassing 0.0001 at 24, 48 and 72 hours, and 0.0016 at 96 hours.

NEW Treatment Affected Cell Adhesion

The alterations in the adhesion capacity of the cells after the 96-hour treatments were assessed. Cells treated with 10% v/v NEW exhibited an adhesion capacity similar to that of control cells ($100\% \pm 26.63$ vs $103.6\% \pm 6.103$, respectively), indicating that their capacity was unaffected. Conversely, adhesion was impacted by NEW concentrations of 20%,

Figure 3: NEW inhibited of MDA-MB-231 cells migration



A) Microphotographs of wound area follow-up in MDA MB-231 cell monolayers at 24, 48, 72 and 96 h of treatment with NEW or doxorubicin. Magnification x 4. B) The graph shows the changes in percentage of reduction in wound area at each monitoring point. It is observed that the wound closes progressively in the control, while the increase in NEW concentration corresponds to wounds that do not decrease their opening area. The P values correspond to significant changes with respect to the control at each follow-up time, * $p<0.5$, ** $p<0.1$, *** $p<0.01$, **** $p<0.001$.

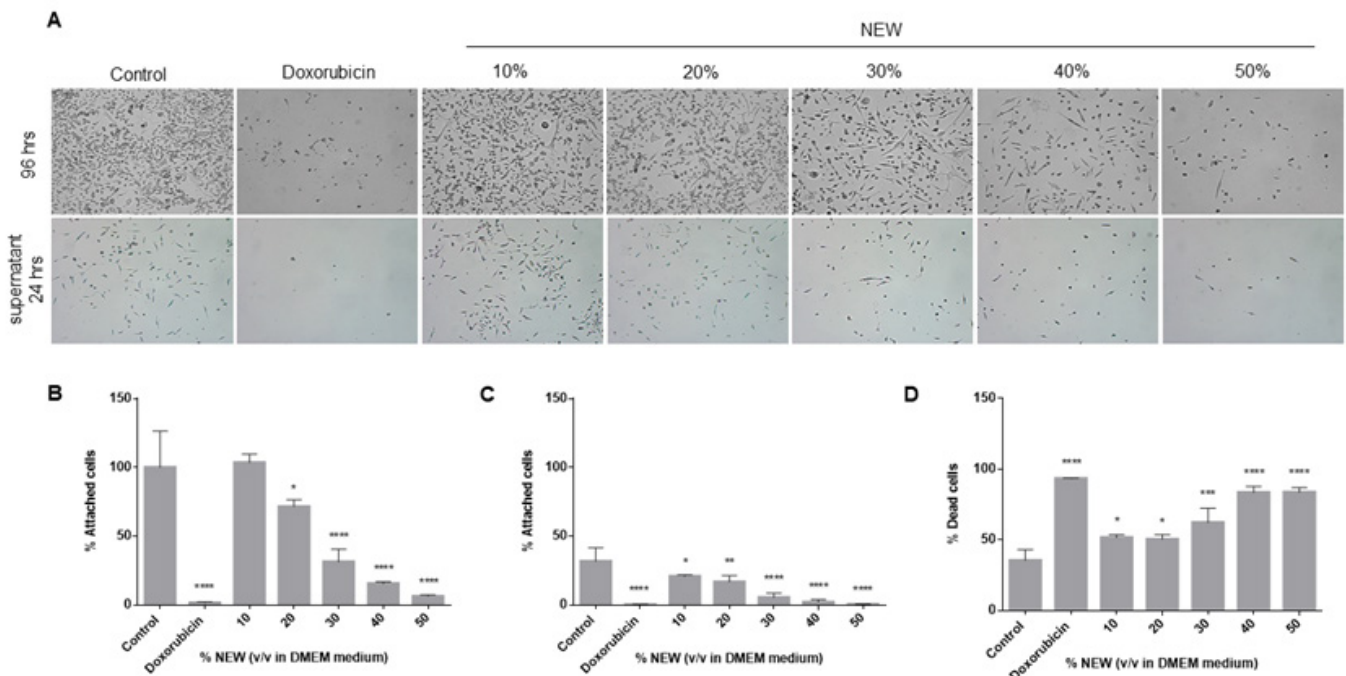
30%, 40% and 50%, with values statistically significant compared to the control. At a concentration of 20%, 71.55%±5.046 of the cells remained adhered to the surface (p=0.0330); at 30%, it was 31.23%±9.443 (p<0.0001); at 40%, it was 15.50%±1.276 (p<0.0001); and at 50%, it was 6.295%±1.110 (p<0.0001). Doxorubicin decreased adhesion to 1.453%±0.7264 (p<0.0001) (Figure 4A, B). Previously, we observed that cells detached during the normal maintenance of the cell line retained adhesion capacity. Given its potential relevance to the metastatic behavior of this subtype of breast cancer, we sought to determine if cells detached after 96 hours of treatment maintained this capacity. The adhesion assessment revealed that cells detached after treatment with 10% of NEW maintained adhesion capacity similar to those detached from untreated monolayers. (Figure 4A, C). Control cells exhibited an adhesion percentage of 31.74%±9.930, while those treated with 10% NEW had 20.71%±1.123 (p=0.0370). In contrast, substrate binding was affected by treatments with 20%, 30%, 40% and 50% of NEW, all exhibiting statistical differences compared to the control. After incubation with the 20% concentration, only 16.79%±4.548 of cells adhered (p=0.0046); at 30%, it was 5.344%±3.291 (p<0.0001); at 40%, it was 2.007%±1.878 (p<0.0001); and at 50%, it was 0.3317%±0.3054 (p<0.0001). The effect of the 50% concentration of NEW was similar to that of doxorubicin, with a percentage value of adhered

cells at 0.11%±0.1928 (Figure 4C). Finally, cell death in this non-adherent cell population was analyzed. For control cells, 35.39%±7.646 of the floating cells were positive for trypan blue staining, while with doxorubicin, it was 93.19%±0.3467 (p<0.0001). The percentages of cell death in cells treated with 10% and 20% of NEW in the medium were statistically different from the control but similar between them, with 51.52%±2.239 (p=0.0133) and 50.35%±3.267 (p=0.0211), respectively. The most significant effects were observed in concentrations higher than 30% of NEW in the medium. The percentage of positive cells staining with trypan blue at the 30% concentration was 62.08%±10.14 (p=0.0002), and at concentrations of 40% and 50%, the values were similar at 83.46%±4.306 (p<0.0001) and 83.51%±3.335 (p<0.0001), respectively (Figure 4D).

NEW Treatment Affected Growth of 3-D Cultures and Inhibited Their Reversion

Spheroids were generated to investigate whether NEW could affect cells in 3D cultures beyond monolayers. After 96 hours of treatment, spheroids were measured, revealing that NEW affected their growth in a concentration-dependent manner (Figure 5). There was no statistical difference between untreated spheroids, which exhibited an average growth of 19.59%±4.108, and 3D cultures treated with 10% NEW, averaging 14.10%±6.118 (p=0.4368). However,

Figure 4: NEW treatment affected cell adhesion



A) The top microphotographs show that after 96 h of treatment there was a decrease in adherent cells proportional to the increase in NEW concentration. The bottom microphotographs show the adherent capacity of the detached cells, which also decreased in correlation with increasing NEW concentrations. Magnification x 10. B) The graph shows the percentage of cells that remained attached after 96 h of treatment. C) The graph shows the percentage of recovered unattached cells that retained adhesion capacity. D) This graph shows the percentage of dead cells, positive for trypan blue, in unattached cells derived from the recovered population. The P values correspond to significant differences compared to control, DMEM medium only, * p<0.5, **p<0.1, *** p<0.01, **** p<0.001.

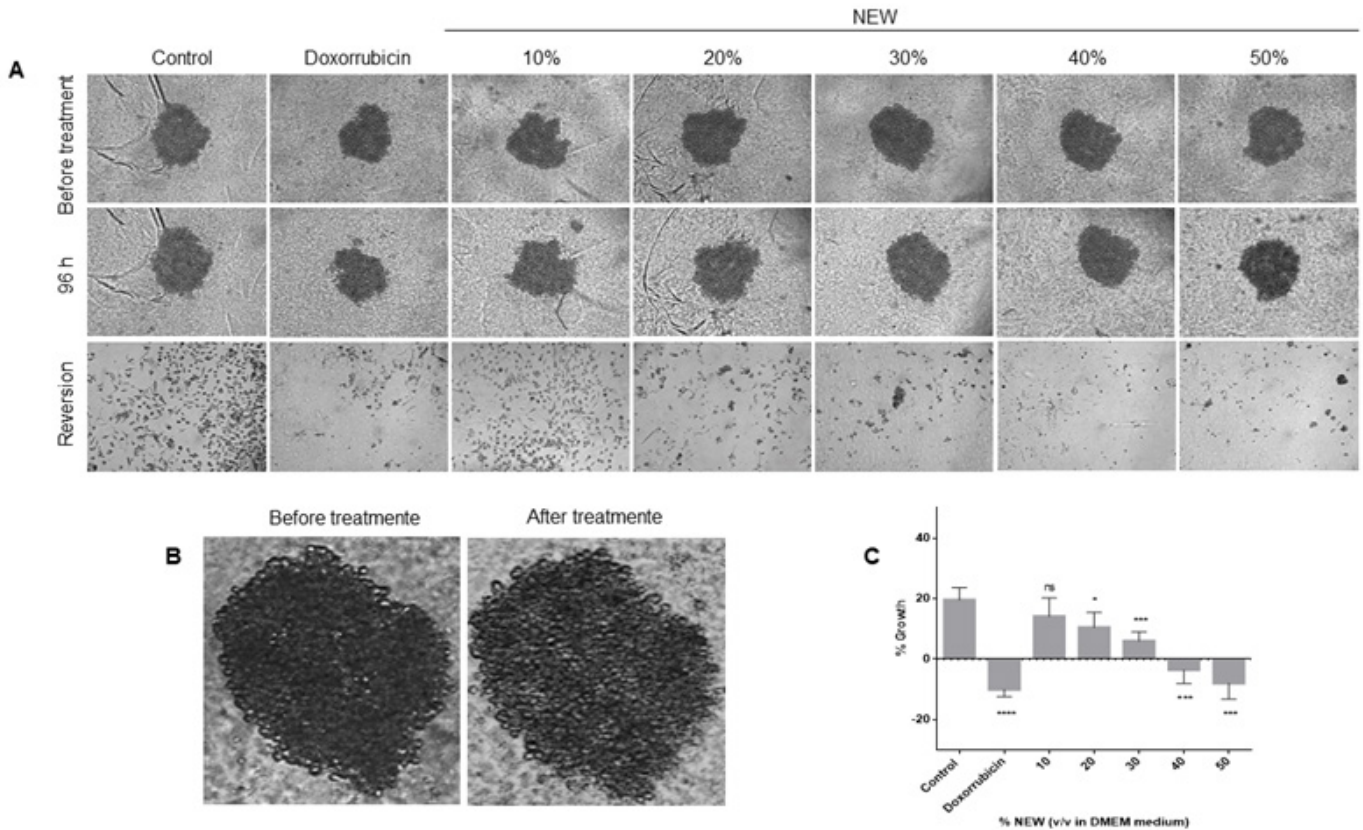
starting from the concentration of 20% NEW, the decrease in growth became significant. Spheroids treated with 20% NEW showed a growth of only 10.460%± 4.999, significantly different from the control with a P value of 0.0203. The changes between 10% and 20% NEW were not different from each other (p=0.7217). Incubation with 30% NEW resulted in spheroids growing only 5.964%±3.056 (p=0.0005 vs control); with 40% NEW, the spheroid size decreased by -3.548%±4.507 (p< 0.0001); and with 50%, the decrease was -7.918±5.329 (p< 0.0001), without a statistical difference between these last two groups (p= 0.6398). Concerning doxorubicin, this treatment decreased the spheroid size by -10.001%±2.374, and this was not significantly different from the effects of 40% and 50% NEW treatments, with P values of 0.3262 and 0.9926, respectively. In other words, the effects of doxorubicin and NEW at 40% and 50% were similar (Figure 5A, C). It is noteworthy that, in addition to the impact on size reduction, structural changes were observed in spheroids treated with NEW at 30% and above, as well as with doxorubicin, where the spheroids appeared less compact and exhibited disorganized borders (Figure 5B). In the reversion assay, we aimed to determine whether cells in

the 3D culture maintained or lost their ability to attach to a substrate and proliferate after NEW treatments. Cells from untreated spheroids adhered, elongated, and displayed their normal morphology in a monolayer when transferred to TC-treated plates (Figure 5A). Cells from spheroids treated with 10% NEW behaved similarly to the control. In contrast, the number of adherent cells dramatically decreased from the 20% NEW concentration. At this NEW concentration in the medium, few adherent cells were observed, and at the concentrations of 30%, 40%, and 50%, none were noticed. These results were similar to those observed in doxorubicin-treated spheroids (Figure 5A).

Discussion

To the best of our knowledge, no previous investigations have systematically examined the impact of neutral electrolyzed water on the viability, migration capacity, adhesion, clonogenic survival, or over 3D cell cultures of MDA-MB-231 cells, representative of a mesenchymal stem-like subtype of triple-negative breast cancer. A prior study reported the inhibition of clonal growth and tumor invasion

Figure 5: NEW treatment decreased growth in 3D cultures and inhibited their reversion



(A) Microphotographs of 3D cultures of MDA-MB-231 that were generated after 72 h of incubation are shown in the top panels. In the middle panel are shown the microphotographs of 3D cultures after 96 h of NEW-treatment. The bottom panels show the microphotographs of the reversion to 2-D cultures. Magnification x 10. It can be seen that starting at the 20% v/v NEW reversion was impaired. In B) a magnification is presented, revealing that the spheroids treated with 50% v/v NEW do not have defined borders and are not compartmentalized. C) The graph corresponds to the changes in spheroid size before and after the treatments.

of human fibrosarcoma cells HT-1080 when treated with reducing electrolyzed water of neutral pH hydrogen-enriched [21]. However, it is crucial to note that the water employed in that study had a distinct composition and physicochemical characteristics compared to the NEW utilized in our research. The HT-1080 cells were exposed to water with an alkaline pH, featuring dissolved hydrogen as the primary component and an ORP of -590 to -104 mV, with subsequent neutralization of pH [21]. In contrast, the NEW used in our study maintains a pH range of 6.5-7.5, with a specified concentration of 0.002% reactive species of chlorine and oxygen, and an oxidation-reduction potential of 750–900 mV. The neutral electrolyzed water under examination induced morphological changes in MDA-MB-231 cells without causing damage to the cell membrane. Moreover, it exhibited concentration-dependent cytotoxic effects on these cells, with a half maximal inhibitory concentration of 28.95% v/v. This observation is noteworthy, especially when considering the limited existing literature on the anticancer effects of electrolyzed water, predominantly those with alkaline pH. In previous studies, it is commonly reported that the cell culture medium was prepared using electrolyzed water instead of ultra-pure water [22,26,27], meaning the cells were exposed to 100% alkaline electrolyzed water. This distinction implies that NEW may demonstrate superior effects on cancer cells compared to alkaline water. The disparities observed can be attributed, as previously mentioned, to differences in composition and physicochemical characteristics, particularly the redox potential, which is extremely low in alkaline water (-600~800 mV) [4].

In studies exploring the anticancer effect of alkaline water, it is postulated that the alteration in cellular redox state is the main mechanism of action, primarily stemming from the presence of dissolved hydrogen [28]. In contrast, NEW contains little to no hydrogen but is abundant in oxidizing species, including hypochlorous acid (HClO) and hydrogen peroxide (H₂O₂), among other reactive oxygen species. Consequently, the mechanism of action of NEW is expected to differ. Both H₂O₂ and HClO have well-documented effects on crucial biological processes in cancer. For instance, through ROS signaling, they modulate the activity of the transcription factor p53, which governs cell growth and proliferation [29]. Furthermore, they influence the transcription factor HIF-1, which regulates gene expression under hypoxic conditions, and the transcription factor NF-κβ, which regulates genes involved in the immune response [30, 31]. Additionally, ROS-mediated signaling plays a role in cell migration, stem cell renewal, tumorigenesis, and epithelial-mesenchymal transition (EMT) [32, 33]. Furthermore, it has been reported that MDA-MB-231 cells exhibit lower capacity to cope with a highly oxidant environment compared to breast adenocarcinoma cell line MCF7 and the non-tumoral breast cell line MCF10A [34]. Hecht et al. demonstrated that

MDA-MB-231 cells are less resistant to extracellular H₂O₂ than non-tumor cells and have an altered intracellular ROS detoxification system, particularly showing lower glutathione peroxidase 1 activity [34]. Similar to H₂O₂, exogenous administration of HOCl has been reported to induce apoptosis in malignant cells [35]. This occurs through a mechanism involving lipid peroxidation and the activation of the mitochondrial pathway of apoptosis [36]. These findings may explain the effect of NEW on MDA-MB-231 viability by a mechanism independent of cell membrane damage. In other words, reactive species present in electrolyzed water could induce oxidative stress in cancer cells, leading to death in a concentration-dependent manner. However, this explanation would not fully account for the changes observed in the other hallmarks of cancer analyzed.

In this regard, we observed that NEW impacts the ability of MDA-MB-231 cells to undergo “unlimited” division and tumor initiation, with the most significant effect observed at the 50% v/v concentration. This suggests that NEW may regulate genes involved in cell cycle progression, proliferation, and immortality, such as p53, p21, PTEN, cyclins, cyclin-dependent kinases or telomerases, and pathways like the PI3K signaling pathway. Notably, Yang et al. reported that H₂O₂ inhibited the proliferation of MDA-MB-231 cells and upregulated p53 expression, inducing apoptosis and G1 or G2/M arrest. This indicates that ROS can indeed regulate these hallmarks of cancer [37]. Although NEW is a complex mixture of ROS, investigations with H₂O₂, the most studied ROS, may provide insights into the possible mechanisms of action of this electrolyzed water in the context of triple-negative breast cancer.

Similarly, NEW affected migration, at concentrations of 30%, 40%, and 50% v/v demonstrated an inhibitory effect from the earliest follow-up time point of 24 hours. This result is noteworthy as it may indicate a direct effect of NEW on this process. Therefore, a detailed analysis of genes associated with cell adhesion and proteolysis, including metalloproteases, integrins, Rho GTPases, among others, should be undertaken. In this context, it has been reported that a sublethal concentration of H₂O₂ inhibited the interaction between DLC1 and caveolin-1 /RhoA signaling, profoundly affecting cell migration in MDA-MB-231 cells [37,38]. Our study findings align with these reports, indicating the negative regulation of ROS in the migration of breast cancer cells. Furthermore, NEW also impacted cell adhesion. At concentrations of 30% v/v and above, cells started to detach from the monolayer, their ability to reattach to a substrate was compromised, and cell death increased compared to untreated cells. The impairment of both adhesion and migration may suggest an effect of NEW on the metastatic potential of this type of triple-negative breast cancer cells. Therefore, it is essential to analyze its effect in *in vivo* models to determine if it could be a therapy that reduces or prevents metastasis. In this

regard, an initial approach is the 3D cell culture model. The observation that no viable cells were seen when NEW-treated spheroids were transferred to adherent surfaces suggests that NEW affected the entire cell pool. This implies that either NEW was able to permeate through the 3D cultures or its effect was transmitted through the surface to the interior of the spheroid, inducing cell death. The results obtained with NEW were comparable to the experimental IC_{50} of doxorubicin (2 μ M), suggesting that 50% v/v NEW has similar effects to the first-line chemotherapeutic in the treatment of triple-negative breast cancer. However, one notable difference was evident between the two treatments. NEW distinctly affected migration at shorter times compared to doxorubicin, which exhibited changes only after 96 hours. Doxorubicin can produce free radicals that induce the generation of H_2O_2 [39]. This reacts with lipids and forms lipid peroxides that destroy the plasma membrane and have been associated with several side effects [39]. As observed in the cell permeability results, doxorubicin-treated monolayers had more staining-positive cells than the highest concentration of NEW tested. This suggests that NEW operates through a different mechanism of cell death and may have fewer adverse effects. In this context, it has been reported that the administration of intratumoral injections of an H_2O_2 -releasing gel, twice a week along with radiotherapy, to patients with locally advanced breast cancer not suitable for surgery, induced a 50% to 100% reduction in tumor volume [40]. The authors suggest that the mechanism by which the shrinkage occurred involves an inflammatory/immune response associated with apoptotic cell death mediated by TRAIL, IL-1b, IL-4, and MIP-1a [40]. In relation to this, oxygen peroxide and hypochlorous acid, the two major active species in NEW, have well-studied roles in the regulation of the antitumor immune response. For example, HOCl is secreted by neutrophils against malignant cells and is involved in the induction of a specific cytotoxic T-cell response [35]. More specifically, the effect of NEW on the regulation of the immune response has recently been established in diseases such as COVID-19, arthritis, nephrotoxicity, and models of Chagas disease [13–18]. Therefore, NEW could be considered a systemic application therapy in cases of triple-negative breast cancer, as it could act directly on tumor cells and modulate the antitumor immune response.

This work has limitations, particularly in that a non-malignant breast cell lineage was not used to determine whether NEW is safe. However, it is important to note that NEW has been approved by the FDA, as it has been demonstrated not to be cytotoxic in fibroblasts. Moreover, it has been shown to not cause skin irritation, systemic, oral or inhalation toxicity, or ocular irritation in animal models, and micronucleus experiments have indicated that it is non-genotoxic [41]. Human studies have further supported its safety, showing no induction of cell damage in human tissues

around wounds or when used for intraperitoneal irrigation nor when it is administered intravenously [15, 42].

Conclusions

Neutral electrolyzed water affected four hallmarks of cancer—cell viability, survival, migration, and adhesion, as well as 3D cultures growing—in a concentration-dependent manner. While the exact mechanism remains unknown, we postulate that the oxygen and chlorine species present in NEW could modulate a series of genes and signaling pathways associated with the development and maintenance of these hallmarks of cancer in addition to increasing oxidative stress. Further studies are necessary to ascertain whether NEW can also affect other characteristics such as DNA synthesis, invasion, tumor metastasis, angiogenesis and chemoresistance. The type of interaction NEW might have with conventional chemotherapeutic agents, whether synergistic or attenuating, and its potential to reduce the adverse effects of these therapies should also be explored.

Authors' contributions

ACL designed the study and carried out data acquisition, JPG conceived the study and carried out data analysis and interpretation, OFBG carried out data acquisition, IDE carried out data analysis and interpretation; BPM participated in the design of the study and interpretation. All authors helped to prepare the manuscript and approved it for submission.

Acknowledgments

To the Esteripharma company for providing the SES for the study

Conflict of interests

Authors Ariana Cabrera-Licona and Brenda A. Paz-Michel declare that they work at the Esteripharma company. Juan Paz-García, Oscar F. Beas-Guzmán and Iván Delgado-Enciso declare no conflict of interest.

References

1. Yahagi N, Kono M, Kitahara M, et al. Effect of Electrolyzed Water on Wound Healing. *Artif Organs* 24 (2000): 984-987.
2. Yan P, Daliri EBM, Oh DH. New Clinical Applications of Electrolyzed Water: A Review. *Microorganisms* 9 (2021): 1-21.
3. Kapur V, Marwaha AK. Evaluation of Effect and Comparison of Superoxidised Solution (Oxum) V/S Povidone Iodine (Betadine). *Indian J Surg* 73 (2011): 48-53.
4. Chen BK, Wang CK. Electrolyzed Water and Its Pharmacological Activities: A Mini-Review. *Molecules* 27 (2022): 1222.

5. Ogunniyi AD, Dandie CE, Brunetti G, et al. Neutral electrolyzed oxidizing water is effective for pre-harvest decontamination of fresh produce. *Food Microbiol.* 93 (2021): 103610.
6. Torres-Rosales E, Rivera-García A, Rosario-Perez PJ, et al. Application of Neutral Electrolyzed Water on pork chops and its impact on meat quality. *Sci Rep* 10 (2020): 19910.
7. Medina-Gudiño J, Rivera-García A, Santos-Ferro L, et al. Analysis of Neutral Electrolyzed Water anti-bacterial activity on contaminated eggshells with *Salmonella enterica* or *Escherichia coli*. *Int J Food Microbiol* 320 (2020): 108538.
8. Velazquez-Meza ME, Hernández-Salgado M, Sánchez-Alemán MA. Evaluation of the Antimicrobial Activity of a Super Oxidized Solution in Clinical Isolates. *Microb Drug Resist* 21 (2015): 367-372.
9. Thorn RM, Lee SWH, Robinson GM, et al. Electrochemically activated solutions: evidence for antimicrobial efficacy and applications in healthcare environments. *Eur J Clin Microbiol Infect Dis* 31 (2012): 641-653.
10. Sipahi H, Reis R, Dinc O, et al. In vitro biocompatibility study approaches to evaluate the safety profile of electrolyzed water for skin and eye. *Hum Exp Toxicol* 38 (2019): 1314-1326.
11. Gutierrez A. The science behind stable, super-oxidized water: Exploring the various applications of super-oxidized solutions. *Wounds* 18 (2006): 7-10.
12. Reis R, Sipahi H, Dinc O, et al. Toxicity, mutagenicity and stability assessment of simply produced electrolyzed water as a wound healing agent in vitro. *Hum Exp Toxicol* 40 (2021): 452-463.
13. Singal R, Zaman M, Singh B, et al. Comparative evaluation of intra-operative peritoneal lavage with super oxidized solution and normal saline in peritonitis cases; randomized controlled trial. *Maedica (Bucur)* 11 (2016): 277-285.
14. Montesinos-Peña NE, Hernández-Valencia M, Delgado-Enciso I, et al. Evaluation of an antiseptic gel of intravaginal application for multitreated patients for infectious cervicovaginitis. *Ginecol Obstet Mex* 87 (2019): 454-466.
15. Delgado Enciso I, Paz García J, Barajas Saucedo CE, et al. Safety and efficacy of a COVID 19 treatment with nebulized and/or intravenous neutral electrolyzed saline combined with usual medical care vs. usual medical care alone: A randomized, open label, controlled trial. *Exp Ther Med* 22 (2021): 1-16.
16. Aurelien-Cabezas NS, Paz-Michel BA, Jacinto-Cortes I, et al. Protective Effect of Neutral Electrolyzed Saline on Gentamicin-Induced Nephrotoxicity: Evaluation of Histopathologic Parameters in a Murine Model. *Medicina (Kaunas)* 59 (2023): 397.
17. Rodríguez-Morales O, Cabrera-Mata JJ, Carrillo-Sánchez SDC, et al. Electrolyzed Oxidizing Water Modulates the Immune Response in BALB/c Mice Experimentally Infected with *Trypanosoma cruzi*. *Pathogens* 9 (2020) 1-20.
18. Rodríguez-Morales O, Mendoza-Téllez EJ, Morales-Salinas E, et al. Effectiveness of Nitazoxanide and Electrolyzed Oxidizing Water in Treating Chagas Disease in a Canine Model. *Pharmaceutics* 15 (2023): 1479.
19. Fremd C, Jaeger D, Schneeweiss A. Targeted and immunobiology driven treatment strategies for triple-negative breast cancer: current knowledge and future perspectives. *Expert Rev Anticancer Ther* 19 (2019): 29-42.
20. Yin L, Duan JJ, Bian XW, et al. Triple-negative breast cancer molecular subtyping and treatment progress. *Breast Cancer Res* 22 (2020): 61.
21. Saitoh Y, Okayasu H, Xiao L, et al. Neutral pH hydrogen-enriched electrolyzed water achieves tumor-preferential clonal growth inhibition over normal cells and tumor invasion inhibition concurrently with intracellular oxidant repression. *Oncol Res* 17 (2008): 247-255.
22. Frajese GV, Benvenuto M, Mattera R, et al. Electrochemically Reduced Water Delays Mammary Tumors Growth in Mice and Inhibits Breast Cancer Cells Survival In Vitro. *Evid Based Complement Alternat Med* 2018 (2018): 4753507.
23. Gebäck T, Schulz MMP, Koumoutsakos P, et al. TScratch: A novel and simple software tool for automated analysis of monolayer wound healing assays: Short Technical Report. *Biotechniques* 46 (2009): 265-274.
24. Metzger W, Sossong D, Bächle A, et al. The liquid overlay technique is the key to formation of co-culture spheroids consisting of primary osteoblasts, fibroblasts and endothelial cells. *Cytotherapy* 13 (2011): 1000-1012.
25. Yakavets I, Francois A, Benoit A, Merlin JL, Bezdetnaya L, Vogin G. Advanced co-culture 3D breast cancer model for investigation of fibrosis induced by external stimuli: optimization study. *Sci Rep* 10 (2020): 21273.
26. Ye J, Li Y, Hamasaki T, et al. Inhibitory effect of electrolyzed reduced water on tumor angiogenesis. *Biol Pharm Bull* 31 (2008): 19-26.
27. Nakamura K, Muraoka O. Effect of electrolyzed water produced using carbon electrodes on HeLa cell proliferation. *Biosci Trends* 11 (2018): 688-693.

28. LeBaron TW, Sharpe R, Ohno K. Electrolyzed-Reduced Water: Review I. Molecular Hydrogen Is the Exclusive Agent Responsible for the Therapeutic Effects. *Int J Mol Sci* 23 (2022): 14750.
29. Liu B, Chen Y, St Clair DK. ROS and p53: a versatile partnership. *Free Radic Biol Med* 44 (2008): 1529-1535.
30. Simon MC. Mitochondrial reactive oxygen species are required for hypoxic HIF alpha stabilization. *Adv Exp Med Biol* 588 (2006): 165-170.
31. Gloire G, Legrand-Poels S, Piette J. NF-kappaB activation by reactive oxygen species: fifteen years later. *Biochem Pharmacol* 72 (2006): 1493-1505.
32. Dickinson BC, Chang CJ. Chemistry and biology of reactive oxygen species in signaling or stress responses. *Nat Chem Biol* 7 (2011): 504-511.
33. Holmström KM, Finkel T. Cellular mechanisms and physiological consequences of redox-dependent signalling. *Nat Rev Mol Cell Biol* 15 (2014): 411-421.
34. Hecht F, Cazarin JM, Lima CE, et al. Redox homeostasis of breast cancer lineages contributes to differential cell death response to exogenous hydrogen peroxide. *Life Sci* 158 (2016): 7-13.
35. Bauer G. HOCl and the control of oncogenesis. *J Inorg Biochem* 179 (2018): 10-23.
36. Bauer G. HOCl-dependent Singlet Oxygen and Hydroxyl Radical Generation Modulate and Induce Apoptosis of Malignant Cells. *Anticancer Res* 33 (2013): 3589.
37. Yang B, Zhu W, Zheng Z, et al. Fluctuation of ROS regulates proliferation and mediates inhibition of migration by reducing the interaction between DLC1 and CAV-1 in breast cancer cells. *In Vitro Cell Dev Biol Anim* 53 (2017): 354-362.
38. Ma L, Zhu WZ, Liu TT, et al. H₂O₂ inhibits proliferation and mediates suppression of migration via DLC1/RhoA signaling in cancer cells. *Asian Pac J Cancer Prev* 16 (2015): 1637-1642.
39. Horenstein MS, Vander Heide RS, L'Ecuyer TJ. Molecular basis of anthracycline-induced cardiotoxicity and its prevention. *Mol Genet Metab* 71 (2000): 436-444.
40. Nimalasena S, Gothard L, Anbalagan S, et al. Intratumoral Hydrogen Peroxide With Radiation Therapy in Locally Advanced Breast Cancer: Results From a Phase 1 Clinical Trial. *Int J Radiat Oncol Biol Phys* 108 (2020): 1019-1029.
41. Aras A, Karaman E, Çim N, et al. The effect of super-oxidized water on the tissues of uterus and ovary: An experimental rat study. *Eastern J Med* 22 (2017): 15-19.
42. Eftekhari-zadeh F, Dehnavieh R, Noori Hekmat S, et al. Health technology assessment on super oxidized water for treatment of chronic wounds. *Med J Islam Repub Iran* 30 (2016): 384.